A New Energetically Optimized Power Supply System for a Mobile Robot Platform, using Ultracapacitors and Batteries to Ensure Both Ultra-fast Charging and Autonomy

Carlos Arantes[1], João Sena Esteves[2] and João Sepúlveda[2]
[1]*Department of Industrial Electronics, University of Minho, Campus of Azurém, 4800-058 Guimarães, Portugal*
[2]*Centre Algoritmi, Department of Industrial Electronics, University of Minho, Campus of Azurém, 4800-058 Guimarães, Portugal*

Keywords: Ultracapacitors, Batteries, Fast Electric Charger, Mobile Robot Platform, Energy Management.

Abstract: The smallest charging times required by fully discharged conventional batteries are some tens of minutes. This is an important limitation for mobile robot platforms. A previous paper already validated the possibility of integrating ultracapacitors and batteries in the same system. However, it has some significant limitations: 1) It works with an ultracapacitors module or a battery, but it does not work with both devices at the same time; 2) It requires an external dedicated charging station; 3) It is not possible to take profit from a part – which is non-negligible – of the energy previously stored in the ultracapacitors. This paper presents a new power supply system for mobile robot platforms that has been developed in order to overcome these limitations. Its main goals are evaluating the feasibility of: 1) Fully integrating batteries and ultracapacitors, working simultaneously as energy-storing devices, with the aim of enabling a mobile robot platform to achieve a reasonable autonomy after a very reduced charging time and considerable autonomy when there are no charging time constraints; 2) Installing all the system in the mobile robot platform, avoiding the use of an external dedicated charging station; 3) Extracting almost all the energy previously stored in the ultracapacitors. Both simulation results and experimental results are presented.

1 INTRODUCTION

Even with fast charging techniques, the smallest charging times required by fully discharged conventional batteries are some tens of minutes, due to the allowable values of their charging currents. An ultra-fast nickel-cadmium battery charger presented by Petchjatuporn *et al.* (2005) took about 13 minutes to fully charge a battery at a C-rate of 8C. This C-rate is so high that it considerably reduces the lifespan of the battery. A research on fast charging for lead-acid batteries was conducted by Siguang *et al.* (2009): charging starts at a C-rate of 1C and then goes decreasing as the battery is being charged, taking at least a couple of hours to fully charge the battery. Batteries charging times of some tens of minutes are an important limitation for mobile robot platforms. It is not possible to work around this limitation by increasing charging currents, since this procedure would rise the temperature too much, deteriorating the batteries.

An interesting possibility would be replacing batteries by ultracapacitors, which allow charging and discharging currents substantially higher than those allowed by common batteries. By that way, their charging periods may be much smaller than those required by batteries and they are able to provide power peaks of significant value. However, using ultracapacitors as the only energy-storing device in mobile robot platforms is not feasible, due to the severe limited achievable autonomy (Muffoletto *et al.,* 2010).

Several applications integrating batteries and ultracapacitors on the same system are currently available (Schneuwly and Gallay, 2000; Awerbuch and Sullivan, 2010; Haifeng and Xueyu, 2010; Niemoeller and Krein, 2010; Monteiro *et al.,* 2011; Qin and Zhu, 2011; Musat *et al.,* 2012). This integration results from the need of having a single power supply system capable of, simultaneously: 1) Storing large amounts of energy in the batteries for the sake of autonomy; 2) Providing power peaks of short duration but significant value using the ultracapacitors, extending the battery lifespan

Arantes C., Sena Esteves J. and Sepúlveda J..
A New Energetically Optimized Power Supply System for a Mobile Robot Platform, using Ultracapacitors and Batteries to Ensure Both Ultra-fast Charging and Autonomy.
DOI: 10.5220/0005531201550163
In *Proceedings of the 12th International Conference on Informatics in Control, Automation and Robotics* (ICINCO-2015), pages 155-163
ISBN: 978-989-758-122-9

(Musat *et al.,* 2012) and/or ensuring the proper functioning of the system (Schneuwly and Gallay, 2000; Monteiro *et al.,* 2011).

A previous paper by Arantes *et al.,* (2014) also validates the possibility of integrating ultracapacitors and batteries in the same system. The main goal of the suggested integration is enabling a mobile robot platform to achieve 1) a reasonable autonomy after a very reduced charging time, when its energy-storing devices (batteries and ultracapacitors) become discharged and there is not enough time to properly charge the batteries; 2) a considerable autonomy when there are no charging time constraints. The power supply system presented in that paper achieved satisfactory results but it has some important limitations, namely:

- It works with an ultracapacitors module or a battery, but it does not work with both devices at the same time. It must be shut down in order to switch the power sources;
- It requires an external dedicated charging station. In fact, some of its components are external to the mobile robot platform, for example a heavy 1500VA/50Hz power transformer;
- It is impossible to extract the energy stored in the ultracapacitors module whenever its voltage becomes under 1.5V. Therefore, it is not possible to take profit from a part of the energy previously stored in that device. In some applications – for example, the one described by Kularatna and Patel (2014) – the ultracapacitors non-extractable energy may be non-negligible.

This paper presents a new power supply system that has been developed in order to overcome these limitations. Its main goals are evaluating the feasibility of:

- Fully integrating batteries and ultracapacitors, working simultaneously as energy-storing devices, to enable a mobile robot platform to achieve a reasonable autonomy after a very reduced charging time and large autonomy when there are no charging time constraints;
- Installing all the system in the mobile robot platform, avoiding the use of an external dedicated charging station;
- Extracting almost all the energy previously stored in the ultracapacitors.

The new power supply system is described in Section 2. The simulation results presented in Section 3 were performed before implementing the physical system described in Section 4. The experimental results presented in Section 5 were obtained with the real system implementation. Section 6 provides the general conclusions and some considerations regarding future developments.

2 SYSTEM ARCHITECTURE OVERVIEW

The new power supply system has four main components:

- **The energy-storing devices**, which are an ultracapacitors module (116F, 16V, 4.12Wh) and a lead-acid battery (12V, 12Ah, 144Wh);
- **The charger**, used to transfer energy from the electrical grid to the energy-storing devices;
- **The energetically optimized voltage regulator**, whose function is to manage the available energy on the energy-storing devices, ensuring 12.5V on its output;
- **The output voltage regulator**, used to supply a regulated voltage to each part of the mobile robot platform from de 12.5V established by the energetically optimized voltage regulator.

2.1 The Charger

Figure 1 shows the block diagram of the subsystem that uses the charger. It is able to charge the ultracapacitors module and the lead-acid battery, one at a time. Firstly, when the charger is turned on (by connecting it to the electrical grid), it injects current on the ultracapacitors module as quickly as possible (the maximum current value is 14A and the maximum output power value is 80W) in order to ensure ultra-fast charging. The ultracapacitors charge process is considered completed when the voltage goes up to 15.5V. Secondly, when the ultracapacitors module is charged, the charger injects 1.2A on the lead-acid battery while the voltage does not go up to 13.8V. Thirdly, when the battery voltage achieves 13.8V, the charger keeps that voltage level constant until the current goes down to 50mA. Finally, when 50mA are achieved, the battery charging process is considered done.

The charger is fed by a 100VA, 50Hz, 230V to 24V single phase toroidal transformer. This transformer was chosen because the maximum output power of the charger is 80W and, in the majority of European countries, the characteristics of single-phase standard electric plugs are 230V AC, 50Hz and 16A (which means 3.45kVA). The transformer is followed by a full-bridge rectifier, which is constituted by 4 schottky diodes MBR1660, and a 10mF capacitive filter. This set of components is responsible for converting the alternating voltage

(230V AC) in approximately 34V DC unregulated. Based on these characteristics, by demanding the maximum power, the expected output voltage ripple is around $15V_{PP}$. Due to the high transformer impedance (when compared to the electrical grid impedance), it was not necessary to develop a circuit to avoid the high values of the start-up current.

A step-down DC-DC converter, working as a pulse width modulation current-controlled voltage source, is the power electronics converter used to convert the input unregulated voltage (34V DC) to an adjustable output current. The step-down DC-DC converter switches at 1kHz. The control system is a regular PI (proportional + integral) controller with a sampling frequency of 4kHz, a proportional gain (Kp) of 40 and an integral gain (Ki) of 100. Figure 2 shows the step-down model developed with PSIM simulation software.

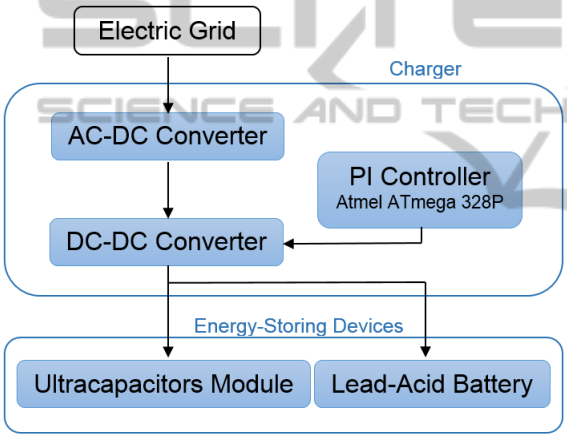

Figure 1: Block diagram of the charger.

In the converter shown in Figure 2, the PI controller manages the duty-cycle applied to the MOSFET MOS1. When the value of the output current is lower than the desirable, the duty-cycle of the PWM signal is increased. When the value of the output current is higher than the desirable, the duty-cycle of the PWM signal is decreased. The PI controller also manages the state of the switches S1 and S2. When it is necessary to charge the ultracapacitors module, S1 is opened and S2 is closed. On the other hand, when it is necessary to charge the lead-acid battery, S1 is closed and S2 is opened. Figure 2 also shows that the two switches (S1 and S2) are in series with the coil L1. Because of that, the PI controller can only change the state of the switches when the current in the coil L1 is null. If this procedure was not followed, it would appear an overvoltage spike in the switch that opened. The diode D1 is the schottky MBR1660, which is used to ensure the path to the current when the MOSFET MOS1 (P80PF55) is turned off. The current rating of the switches S1 and S2 is 16A. The coil L1 is used to smooth the output current and it has 23.12mH, 428mΩ at 1kHz.

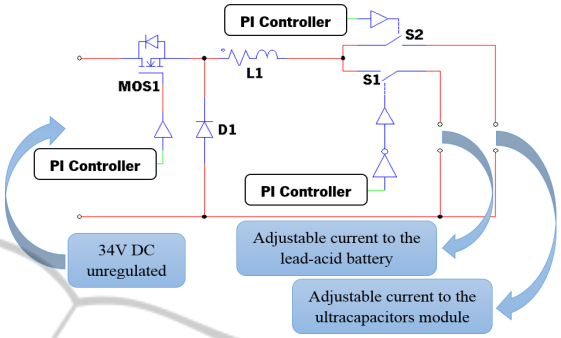

Figure 2: PSIM model of the step-down of the charger.

2.2 The Energetically Optimized Voltage Regulator

Figure 3 shows the block diagram of the subsystem that uses the energetically optimized voltage regulator. Its main goal is to manage the available energy on the energy-storing devices, ensuring 12.5V on its output. It is considered energetically optimized because, firstly, it uses the energy available on the ultracapacitors module to ensure 12.5V on its output and, secondly, when there is not enough energy on the ultracapacitors module, it uses the energy available on both energy-storing devices to ensure 12.5V. This architecture has the following advantages:

- **Increasing the Battery Lifespan**. The fact of using, in first place, the energy stored on the ultracapacitors module leads to a lower battery usage;
- **Reducing the Frequency of the Battery Replacement**. The increased battery lifespan leads to a reduction of the number of times that the battery needs to be replaced in a specific time period. In a long term, this fact may mean the reduce of the cost of the system in which the battery is installed;
- **Due to the Use of Two Energy-storing Devices, the Ultracapacitors Module can be Fully Charged and Fully Discharged**. So, there is a better use of the ultracapacitors module storage capacity.

To do the development, it was defined that the mobile robot platform could demand up to 6A at 12V. Because of that, the energetically optimized voltage regulator was designed to ensure a maximum current value of 6A on its output. The

reason why it was chosen 12.5V on its output instead of 12V is related to the voltage regulator architecture. The step-up converter does not have the ability to block the energy flow from its input to its output when the output voltage is lower than the input voltage. When the battery is fully charged, its voltage may go up to 12.5V. Therefore, using this architecture, the way to block the energy flow (when it is desirable) is ensuring that the output voltage is always equal or greater than the input voltage.

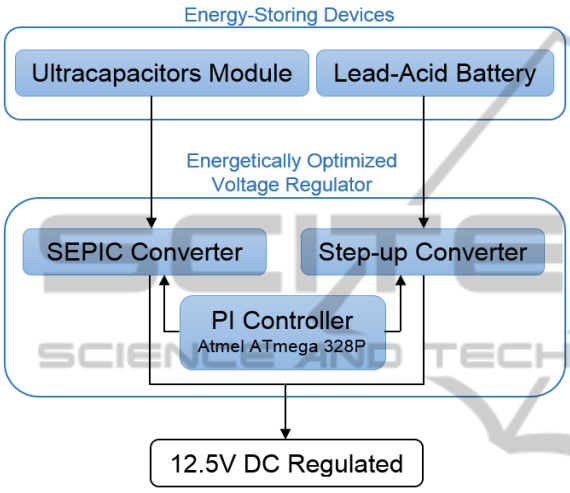

Figure 3: Block diagram of the subsystem that uses the energetically optimized voltage regulator.

The energetically optimized voltage regulator model, developed with PSIM simulation software, is shown in Figure 4. It is based on the SEPIC (Single-Ended Primary-Inductor Converter) and step-up converters. The outputs of the two converters are in parallel and, because of that, the ground is the same for both. The coils L1 and L2 have 42,7µH and 95mΩ at 1kHz. The coil L3 has 244µH and 102mΩ at 1kHz. The MOSFETs MOS1 and MOS2 are the P60NF06. The diodes D1 and D2 are the schottky MBR1660. The capacitor C1 has 10µF and the capacitor C2 has 1mF.

When there is available energy on the ultracapacitors module, the MOSFET MOS1 is switched by a PI controller in order to keep the output voltage regulated on 12.5V. In this case, the energy only comes from the ultracapacitors module and the MOSFET MOS2 is turned off. When the energy on the ultracapacitors module is not enough to keep the output voltage regulated at 12.5V, the MOSFET MOS1 switches with 85% of duty-cycle and the MOSFET MOS2 switches with an adjustable duty-cycle. In this case, the energy comes from both energy-storing devices to the output.

The computation of the PWM signal applied to the MOSFETs MOS1 and MOS2 is based on a PI controller with an extended output. The MOSFET MOS1 handles a maximum duty-cycle of 85% and the MOSFET MOS2 handles a duty-cycle value that is given by the difference between the computed value and 85%. For example, if the computed output of the PI controller is 135, the duty-cycle of MOSFET MOS1 will be 85% and the duty-cycle of MOS2 will be 50%. The maximum duty-cycle on each MOSFET is 85%. Therefore, the saturation value of the PI controller is 170. The input of the PI controller is the voltage on the output of the voltage regulator. When its value is lower than the desirable, the duty-cycle is increased. When its value is higher than the desirable, the duty-cycle is decreased.

The PI controller has a proportional gain of 15 and an integral gain of 250. The sampling frequency is about 4kHz and the switching frequency (applied to the MOSFETs) is about 9.8kHz.

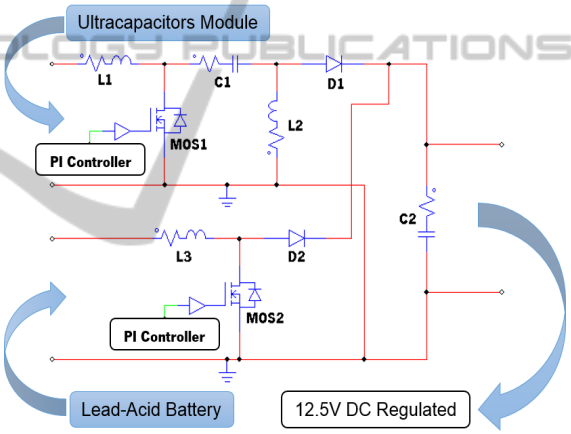

Figure 4: PSIM model of the energetically optimized voltage regulator.

2.3 The Output Voltage Regulator

Figure 5 shows the block diagram of the subsystem that uses the output voltage regulator. Its main function is to supply a regulated voltage to the four brushed DC motors of the mobile robot platform from the 12.5V DC regulated (imposed by the energetically optimized voltage regulator).

The output voltage regulator is based on four independent full H-bridges. The input of each full H-bridge is the 12.5V DC regulated and each one is used to supply each brushed DC Motor of the mobile robot platform. It is used a PWM signal to control the state of each MOSFET of each bridge. The rotation direction, the angular velocity and the torque of each brushed DC motor are managed by a

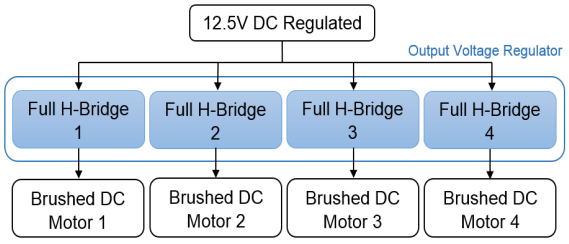

Figure 5: Block diagram of the output voltage regulator.

MRP (Mobile Robot Platform) controller. This controller computes, for each instant, the average voltage that should be supplied to each motor. Based on this calculation, it is done a conversion from the average voltage to the duty-cycle of the PWM signal. It is used bipolar modulation, which means that MOSFETs work in pairs – when the duty-cycle is 100%, the average output voltage is 12.5V and when the duty-cycle is 0%, the average output voltage is -12.5V.

Figure 6 presents the topology used to supply each motor. Each motor has a rated voltage of 12V and a maximum current of 1.5A. Because of that, it was used two L298 integrated circuits to implement the four full H-bridges.

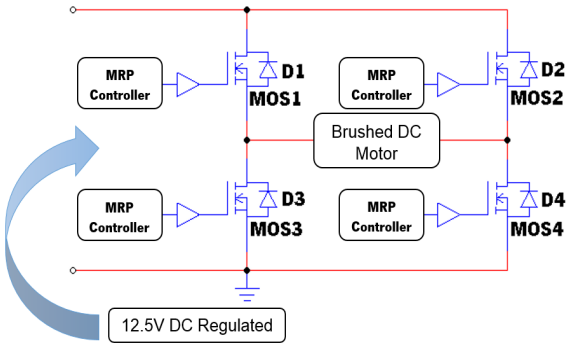

Figure 6: PSIM model of the output voltage regulator.

3 SIMULATION RESULTS

It was used the PSIM simulation software to validate all the developed blocks of the power supply system. Using this software it was possible to analyse the expected system performance and to prevent design mistakes before any circuit implementation, as well as making adjustments to the gains of the PI controllers to achieve a better overall system performance. The most important simulations results are presented in this section.

3.1 The Charger

The charger was simulated when it is feeding the ultracapacitors module. A maximum output power of 80W, a maximum output current of 14A and a final voltage of 15.5V were considered. Figure 7 shows that the ultracapacitors module charging process is performed successfully. It is also shown that, when the ultracapacitors module is charged, the system begins to charge the lead-acid battery.

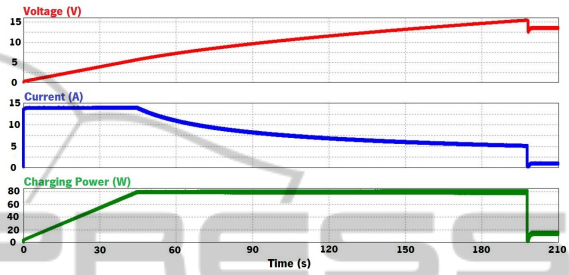

Figure 7: PSIM simulation results of the charger when it is charging the ultracapacitors module up to 15.5V.

3.2 The Energetically Optimized Voltage Regulator

The energetically optimized voltage regulator was simulated supplying a 12.5V, 1A load. It was considered that the ultracapacitors module and the battery were fully charged. In Figure 8 it is noticed that the circuit draws more current from the ultracapacitors module as its voltage drops, in order to keep constant the output power. Furthermore, it is shown that the energetically optimized voltage regulator is able to take energy from the battery when the voltage on the ultracapacitors module drops too much and it is able to take almost all the energy available on the ultracapacitors module.

3.3 The Output Voltage Regulator

The output voltage regulator was simulated considering an input voltage of 12.5V (it is the output of the energetically optimized voltage regulator), a duty-cycle of 75% and an inductive load of 6Ω and 500µH. This simulation is important to check the voltage and current behaviour when the output voltage regulator is supplying a DC brushed motor (it is an inductive load with electromotive force). In Figure 9 it is visible that the output voltage is a square ware, with a maximum of 12.5V and a minimum of -12.5V, where the average output voltage depends of the duty-cycle. In spite of the usage of an output square wave (it is constantly

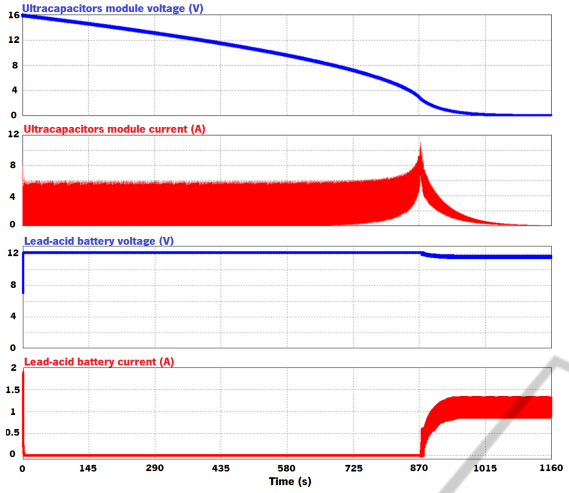

Figure 8: PSIM simulation results of the energetically optimized voltage regulator when it is providing 12.5V, 1A on its output.

changing), there are no problems to DC brushed motors because current is filtered by its inductance and switching intervals are much shorter than the mechanical time constants involved.

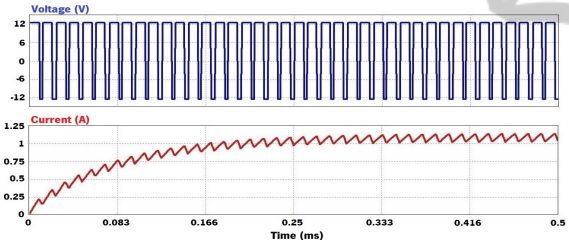

Figure 9: PSIM simulation results of load voltage and current when the output voltage regulator has a duty-cycle of 75% and an input voltage of 12.5V.

4 SYSTEM IMPLEMENTATION

Section 4 presents a detailed description of the real system implementation. It was done after having simulated and validated all the system architecture by using the PSIM simulation software.

4.1 Hardware

The charger is able to charge both energy storing devices. It charges the ultracapacitors module in first place and then it charges the lead-acid battery. This strategy was followed so as to ensure ultra-fast charging (reducing at minimum the charging time). The charger hardware was fully mounted onboard the mobile robot platform to ensure that whenever it is necessary to charge, no external additional hardware is needed – Unlike a previous work by Arantes *et al.,* (2014), the charger does not need of a dedicated charging station. The hardware implementation was made by developing a printed circuit board (PCB) using the CadSoft Eagle 6.4.

The energetically optimized voltage regulator is capable of providing 12.5V on its output from the energy available on both energy storing devices. Its PCB implementation can be seen in Figure 10. That Figure also shows the final implementation of the whole power supply system: the charger, the energetically optimized voltage regulator and the output voltage regulator. The output voltage regulator is able to provide the suitable average voltage for each brushed DC motor ensuring that the mobile robot platform moves to where is required. That voltage is computed by the MRP controller, which is based on the Atmel ATmega 1284P microcontroller.

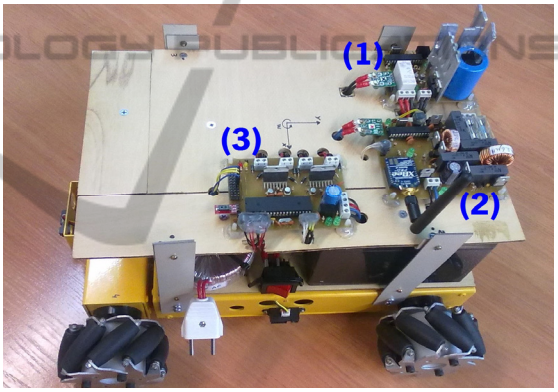

Figure 10: Final version of the mobile robot platform. It is visible the whole power supply system: the charger PCB (1), the energetically optimized voltage regulator PCB (2) and the output voltage regulator PCB (3).

4.2 Software

The charger is capable of charging both energy storing devices. For each time instant, the operation mode of the charger is dependent of the energy storing device that is being charged. The output current and voltage of the charger are managed by the algorithm that was described in Section 2.

The energetically optimized voltage regulator uses a non-conventional digital PI controller, which was implemented on another Atmel ATMega 328P microcontroller. Its main particularity is the fact that it has an extend output to deal with both SEPIC and step-up converts. According to the algorithm, for a computed duty-cycle equal or lower than 85%, it is switched only the SEPIC converter. For higher duty-

cycle values, both converters are switched having in account that, for each converter, the duty-cycle value can never be higher than 85%. If that precaution was not taken, due to the nature of the circuit, the power converters could be destroyed by a short circuit.

The output voltage regulator takes the 12.5V from the energetically optimized voltage regulator and provides the suitable average voltage for each brushed DC motor of the mobile robot platform. It was implemented a digital PID controller to ensure that each wheel of the mobile robot platform has a measured velocity that closely follows a reference velocity specified by the MRP controller, whose main function is to define the trajectories of the mobile robot platform. The algorithm of the output voltage regulator was implemented on an Atmel ATmega 1284P microcontroller.

All the Atmel ATmega microcontrollers used on the power supply system were programmed using the Atmel Studio 6.1 software.

5 EXPERIMENTAL RESULTS

Some experimental tests were made to ensure the correct operation of each component of the system and to further validate the proposed topology.

5.1 The Charger

The charger module was tested by charging the two energy-storing devices. By considering only theoretical calculations, the expected charging time for the ultracapacitors module was, approximately, 3 minutes and 20 seconds. Because the charging current is limited to a maximum of 14A, the maximum charging power (80W) was only achieved when the voltage in the ultracapacitors module reached 5.7V. The practical results showed that the real charging time is 3 minutes and 42 seconds. The cause of the time gap between theoretical and practical results is the fact that theoretical calculations did not consider all the circuit losses and parasitic effects. Some of them are very hard and require very expensive equipment to be assessed. The ultracapacitors module charging was considered done when its voltage reached 15.5V. After that, the lead-acid battery charging proceeded. The measured charging time for the battery was approximately 8 hours and 30 minutes.

5.2 The Energetically Optimized Voltage Regulator

The main function of this voltage regulator is to ensure 12.5V at its output using the energy available on both the ultracapacitors module and the battery by extracting energy from both of them. For an ultracapacitors module voltage equal or higher than 2.48V, the voltage regulator only uses the energy available on the ultracapacitors module. For an ultracapacitors module voltage lower than 2.48V, the system uses the energy available on both energy storing devices.

It was also found that the energetically optimized voltage regulator is able to extract almost all the energy available on the ultracapacitors module, taking its voltage almost to 0V.

5.3 The Output Voltage Regulator

The output voltage regulator is the last stage of the power supply system of mobile robot platform. Considering both energy storing devices fully charged and running some experimental tests, it was found that, by placing the mobile platform on a flat surface at maximum speed (approximately 60 cm/s), the average autonomy was 23 minutes and 13 seconds using only the available energy on the ultracapacitors module. Using all the available energy on both sources it was achieved an autonomy of approximately 9 hours and 40 minutes.

6 CONCLUSIONS AND FUTURE DEVELOPMENTS

An electrical power supply system for a mobile robot platform has been developed. The system uses ultracapacitors and batteries as energy-storing devices. This paper described a major improvement of a previous work done by Arantes *et al.,* (2014), as the new system is much lighter and more compact, which allowed all of its components to be mounted onboard the mobile robot platform. The system is composed of three modules: 1) a charger and the energy-storing devices; 2) an energetically optimized voltage regulator; 3) an output voltage regulator.

With regard to the charger, the charging time measured for the ultracapacitors module was, approximately, 3 minutes and 42 seconds (starting with a fully-discharged module). Because the charging current is limited to a maximum of 14A,

the maximum charging power (80W) was only achieved when the ultracapacitors module voltage reached 5.7V. The ultracapacitors module charging was completed when its voltage reached 15.5V. After that, the lead-acid battery charging proceeded.

A small disturbance is visible in the voltage and current waveforms at the output of the energetically optimized voltage regulator, considering a power of 12.5W. This is due to the starting of the step-up converter. Until then, only the ultracapacitors module was providing power to the load. Observing the voltage and current waveforms in the ultracapacitors module, it is possible to conclude that the average current value tends to increase due to the decreasing in the average voltage value, as expected, because only then is it possible to maintain a constant output power.

Regarding the practical implementation of the two previous systems, printed circuit boards were implemented using the Eagle Cadsoft 6.4 and digital PI controllers were developed with Atmel Studio 6.1 and microcontrollers Atmel ATmega 328P.

The output voltage regulator is the last stage of the power supply system. It is responsible for supplying the suitable average voltage to the motors of the mobile robot platform. Autonomy tests were made and it was found that, if the mobile robot platform is placed on a flat and horizontal surface at maximum speed (about 60 cm/s), the average autonomy is about 23 minutes and 13 seconds using only the available energy in ultracapacitors module. From that moment, which corresponded to an ultracapacitors module voltage of 2.48V, the system started to use the energy available in both sources and achieved an autonomy of, approximately, 9 hours and 40 minutes. It was verified that the system was able to extract almost all of the energy stored in the ultracapacitors module, taking its voltage almost to 0V. Regarding the practical implementation of this last system, a printed circuit board was also developed through the Eagle Cadsoft 6.4, and a digital PID controller was implemented using the Atmel software Studio 6.1 and the microcontroller Atmel ATmega 1284P.

As a future development, it is suggested to modify the circuits and the control systems in order to allow energy interchange between the ultracapacitors module and the batteries. This will improve energy efficiency in the event that only a fraction of the energy stored in the ultracapacitors module is used.

ACKNOWLEDGEMENTS

This work has been supported by FCT – Fundação para a Ciência e Tecnologia in the scope of the project: PEst-UID/CEC/00319/2013.

REFERENCES

Arantes, C., Sepúlveda, J., Esteves, J., Costa, H., Soares, F., Using Ultracapacitors as Energy-storing Devices on a Mobile Robot Platform Power System for Ultra-fast Charging; *ICINCO 2014, 11th International Conference on Informatics in Control, Automation and Robotics,* 2014, Page(s): 156 – 164, ISBN 978-989-758-040-6. DOI: 10.5220/0005061801560164.

Awerbuch, J. J., Sullivan, C. R., Filter-based Power Splitting in Ultracapacitor-Battery Hybrids for Vehicular Applications; *COMPEL 2010, Control and Modeling for Power Electronics*, 2010, Pages(s): 1 – 8. DOI: 10.1109/COMPEL.2010.5562429.

Bernholc, J., Ranjan, V., Zheng, X. H., Jiang, J., Lu, W., Abtew, T. A., Boguslawski, P., Nardelli, M. B., Meunier, V., Properties of High-Performance Capacitor Materials and Nanoscale Electronic Devices; *HPCMP-UGC 2010, High Performance Computing Modernization Program Users Group Conference*, 2010, Page(s): 195 – 200. DOI: 10.1109/HPCMP-UGC.2010.76.

Haifeng, Dai and Xueyu, Chang; A Study on Lead Acid Battery and Ultra-capacitor Hybrid Energy Storage System for Hybrid City Bus; *ICOIP 2010, International Conference on Optoelectronics and Image Processing*, 2010, Page(s): 154 – 159. DOI: 10.1109/ICOIP.2010.321.

Kularatna, N., Patel, A., Supercapacitors for Energy Mangement in Autonomous Sensor Nodes; *WAC, World Automation Congress,* 2014, Page(s): 604 – 609. DOI: 10.1109/WAC.2014.6936064.

Monteiro, J., Garrido, N., Fonseca, R., Efficient Supercapacitor Energy Usage in Mobile Phones; *ICCE 2011, 2011 International Conference on Consumer Electronics* – Berlin, 2011, Pages(s): 318 – 321. DOI: 10.1109/ICCE-Berlin.2011.6031796.

Muffoletto, D., Mandris, C., Olabisi, S., Burke, K., Zirnheld, J., Moore, H., Singh, H., Design and Analysis of a Smart Power Management System for Ultracapacitor-Powered Robotic Platform; *IPMHVC, Power Modulator and High Voltage Conference,* 2010, Page(s): 643 – 646. DOI: 10.1109/IPMHVC.2010.5958441.

Musat, A. M., Carp, M., Borza, P., Musat, R., Sojref, D., Hybrid Storage Systems and Dynamic Adapting Topologies for Vehiche Applications; *OPTIM 2012, 2012 13th International Conference on Optimization of Electrical and Electronic Equipment*, 2012, Page(s): 1842 – 1566. DOI: 10.1109/OPTIM.2012.6231910.

Niemoeller, B. A. and Krein, P. T., Battery-Ultracapacitor

Active Parallel Interface with Indirect Control of Battery Current; *PECI 2010, Power and Energy Conference at Illinois*, 2010, Pages(s): 12 – 19. DOI: 10.1109/PECI.2010.5437163.

Petchjatuporn, P., Wicheanchote, P., Khaehintung, N., Kiranon, W., Sunat, K., Chiewchanwattana, S., Intelligent ultra-fast charger for Ni-Cd batteries; *ISCAS 2005, IEEE International Symposium on Circuits and Systems*, 2005, Page(s): 5162 – 5165 Vol. 5. DOI: 10.1109/ISCAS.2005.1465797.

Qin, G., Zhu, H., Hybrid Power Supply of Rescue Robot Based on Supercapacitors; *ICMACE 2011, 2th International Conference on Mechanic Automation and Control Engineering,* 2011, Page(s): 1350 – 1353. DOI: 10.1109/MACE.2011.5987194.

Schneuwly, A., Gallay, R., Properties and Applications of Supercapacitors from the State-of-Art to Future Trends; *Proceeding PCIM 2000*, 2000.

Siguang, Li, Chengning, Zhang, Shaobo, Xie, Research on Fast Charge Method for Lead-Acid Electric Vehicle Batteries; *ISA 2009, International Workshop on Intelligent Systems and Applications*, 2009, Page(s): 1 – 5. DOI: 10.1109/IWISA.2009.5073068.